A NUMERICAL SIMULATION OF WIND-DRIVEN BAROCLINIC OCEAN CIRCULATION

Xing Runan (邢如楠)*

Institute of Atmospheric Physics, Academia Sinica, Beijing

Received October 30, 1986

ABSTRACT

A three-level baroclinic ocean model has been developed for studying climate and climatic change. The major large-scale features of temperature field, such as the belt of cold water, strong upwelling and the main currents in the Pacific Ocean, have been reproduced. The simulated results show that the seasonal variation of current is related to that of trade wind system. The simulated equatorial countercurrent is strong in summer and weak even vanished in winter. The south equatorial current, north of the equator is stronger in winter than in summer, but the contrary is the case with the current existing in the Southern Hemisphere.

I. INTRODUCTION

It is well known that the ocean is an inseparable part of the earth climate system. The climate and its change are then associated with the large-scale interaction between the ocean and the atmosphere, thus the research on oceanic dynamics is of importance equivalent to that of atmospheric dynamics.

Of low frequency changes of ocean-atmosphere climate system, seasonal change is the major one. The seasonal change of ocean currents is mainly caused by that of winds. A three-level baroclinic ocean model is formulated in this paper to study the average climate of oceans and the seasonal change of currents.

II. MODEL

The formulation of the model in this paper is based on the primitive equations with the hydrostatic and Bousinesq approximations. The equations of model are as follows:

$$\frac{\partial u}{\partial t}+\frac{\partial (uu)}{\partial x}+\frac{\partial (uv)}{\partial y}+\frac{\partial (uw)}{\partial z}=-\frac{1}{\rho_0}\frac{\partial P}{\partial x}+fv+A_1\nabla^2 u+\frac{\partial}{\partial z}K_1\frac{\partial u}{\partial z}, \tag{1}$$

$$\frac{\partial v}{\partial t}+\frac{\partial (uv)}{\partial x}+\frac{\partial (vv)}{\partial y}+\frac{\partial (vw)}{\partial z}=-\frac{1}{\rho_0}\frac{\partial P}{\partial y}-fu+A_1\nabla^2 v+\frac{\partial}{\partial z}K_1\frac{\partial v}{\partial z}, \tag{2}$$

$$\frac{\partial u}{\partial x}+\frac{\partial v}{\partial y}+\frac{\partial w}{\partial z}=0, \tag{3}$$

* Present affiliation: Beijing Institute of Meteorology, Beijing

$$\frac{\partial P}{\partial z} = -\rho g, \tag{4}$$

$$\rho = \rho_0[1 - \alpha(T - T_0)], \tag{5}$$

$$\frac{\partial T}{\partial t} + \frac{\partial(uT)}{\partial x} + \frac{\partial(vT)}{\partial y} + \frac{\partial(wT)}{\partial z} = A_2\nabla^2 T + h^{-1}\frac{\partial}{\partial z}K_2\frac{\partial T}{\partial z}, \quad h = \begin{cases} 1, & \frac{\partial T}{\partial z} > 0 \\ 0, & \frac{\partial T}{\partial z} \leqslant 0 \end{cases} \tag{6}$$

where A_1 and K_1 are the horizontal and vertical viscosity coefficients, respectively; A_2 and K_2 the horizontal and vertical diffusion coefficients; ρ_0 and T_0, the reference density and temperature of sea water; α is the thermal expansion coefficient of sea water; h indicates the parameterization of free convection, which makes it possible that the strong vertical mixing restores to a neutral stratification whenever the vertical stratification is unstable. The boundary conditions are as follows:

(1) At the lateral boundary

$$V_n = 0, \quad T_x = T_y = 0, \tag{7}$$

where V_n is the velocity normal to the boundary.

(2) At the top ($z=0$)

$$\begin{cases} w = 0, \\ K_1\left(\frac{\partial u}{\partial z}, \frac{\partial v}{\partial z}\right) = \rho_0^{-1}(\tau^x, 0), \\ K_2\frac{\partial T}{\partial z} = Q_s/\rho_0 C_p, \end{cases} \tag{8}$$

where τ^x is the component of wind stress at sea surface in x-direction; C_p is the specific heat of sea water at constant pressure; Q_s is the heat flux downward from the sea surface, and can be expressed as

$$Q_s = Q_2(T_A^* - T_s) \tag{9}$$

according to Haney (1971). Here Q_2 is a coefficient, T_s is the sea surface temperature and T_A^* is the sea surface air temperature

(3) At the bottom ($z=-H$)

$$\begin{cases} w = 0, \\ \frac{\partial u}{\partial z} = \frac{\partial v}{\partial z} = \frac{\partial T}{\partial z} = 0. \end{cases} \tag{10}$$

The model is integrated over a regular basin including equatorial region and a flat bottom. The ocean is divided into three levels: the first level is at 50 m from the sea surface downward, the second at 250 m and the third at 1500 m. The total depth of ocean is taken as 4000 m. The south and north boundaries of integrated domain are at -2750 m and $+4750$ m, respectively. The horizontal width is 10000 km. Grid size is 500 km, all the variables are fixed at a given grid point.

The total velocity is a combination of the vertically mean velocities ($\bar{U}, \bar{V}$) and their deviations ($u' = \bar{U} - u, V' = \bar{V} - v$). $\bar{U}$ and $\bar{V}$ are defined as

$$\overline{(\quad)} = \frac{1}{H}\int_{-H}^{0} (\quad) dz, \tag{11}$$

where H is the total depth of ocean.

If the vertically mean velocity is described by a streamfunction Ψ, we have

$$\bar{U} = -\frac{\partial \Psi}{\partial y}, \tag{12}$$

$$\bar{V} = \frac{\partial \Psi}{\partial x}. \tag{13}$$

In order to calculate the streamfunction Ψ, using Eqs. (1), (2), (11), (12) and (13), we get the vorticity equation

$$\frac{\partial}{\partial t}\nabla^2\Psi = -\beta\frac{\partial \Psi}{\partial x} + A_1\left(\frac{\partial}{\partial x}\nabla^2\bar{V} - \frac{\partial}{\partial y}\nabla^2\bar{U}\right) - \frac{1}{\rho_0 H}\frac{\partial \tau^x}{\partial y} + \left(\frac{\partial \bar{F}}{\partial x} - \frac{\partial \bar{G}}{\partial y}\right), \tag{14}$$

where

$$\nabla^2 = \frac{\partial^2}{\partial x^2} + \frac{\partial^2}{\partial y^2}, \tag{15}$$

$$F = \frac{\partial(uu)}{\partial x} + \frac{\partial(uv)}{\partial y} + \frac{\partial(uw)}{\partial z}, \tag{16}$$

$$G = \frac{\partial(uv)}{\partial x} + \frac{\partial(vv)}{\partial y} + \frac{\partial(vw)}{\partial z}. \tag{17}$$

Table 1. The Parameters Used in the Model

Parameter Value	Unit	Parameter Value	Unit
$\Omega = 7.27\times10^{-5}$	s^{-1}	$A_2 = 2\times10^{8}$	$cm^4\ s^{-1}$
$g = 980$	$cm\ s^{-1}$	$K_2 = 1$	$cm^2\ s^{-1}$
$T = 278.2$	K	$H = 4\times10^5$	cm
$\alpha = 2.0\times10^{-4}$	K^{-1}	$\Delta x = 5\times10^7$	cm
$C = 0.958$	$cal\ g^{-1}\ K^{-1}$	$\Delta y = 5\times10^7$	cm
$\rho_0 = 1.0276$	$g\ cm^3$	$\Delta t = 3600$ (for computing mean velocity)	s
$A_1 = 4\times10^7$	$cm^2\ s^{-1}$		
$K_1 = 1.5$	$cm^2\ s^{-1}$	$\Delta t = 7200$ (for computing deviation velocity)	

Vertical deviation velocity u' and v' are obtained by substracting vertically mean velocity from (1) and (2):

$$\frac{\partial u'}{\partial t} = -\frac{1}{\rho_0}\frac{\partial P'}{\partial x} + fv' + A_1\nabla^2 u' + \frac{\partial}{\partial z}K_1\frac{\partial u'}{\partial z} - \frac{\tau^x}{\rho_0 H} + (F - \bar{F}), \tag{18}$$

$$\frac{\partial v'}{\partial t} = -\frac{1}{\rho_0}\frac{\partial P'}{\partial y} - fu' + A_1\nabla^2 v' + \frac{\partial}{\partial z}K_1\frac{\partial v'}{\partial z} + (G - \bar{G}), \tag{19}$$

where $P' = P - \bar{P}$ is the deviation of P from the vertical mean which can be computed from Eqs. (4) and (11); F and G indicate the advection terms, expressed by Eqs. (16) and (17); w is the vertical velocity which can be evaluated by integrating the continuity equation of from $z = -H$

to z, i.e.

$$w(z) = -\int_{-H}^{z} \left(\frac{\partial u}{\partial x} + \frac{\partial v}{\partial y}\right) dz. \tag{20}$$

The total velocity of ocean currents is equal to the vertically mean velocity plus the deviation from the vertical mean. The parameters used in the model are listed in Table 1.

III. INITIAL CONDITIONS AND NUMERICAL SCHEME

The initial conditions of ocean for numerical modeling are that the ocean remains at rest and has a horizontally homogeneous temperature for each level, taking 25°C, 11°C and 5°C for levels 1, 2 and 3, respectively.

The center-difference scheme is used in the spatial difference and the Lilly scheme with conservation of total energy and momentum is adopted for the computation of horizontal advection terms in the motion equation. By the use of the leapfrog time integration scheme, the diffusion and viscosity terms are evaluated with the aid of forward time difference, but the Coriolis term with aid of the semi-implicit scheme. In calculating the vertically mean velocity, the time step Δt is taken to be 3600 s and the variables at each time step are averaged over three consecutive ones, meanwhile, an Eular backward time integration scheme and spatial smoothing are performed every five time steps, and a forward time difference every six ones. While in calculating the deviation velocity with taking $\Delta t = 7200$ s, the Eular backward scheme is performed every ten time steps, and time smoothing every six ones.

The direct method, as described by Veronis (1966), is utilized to solve the Poisson equation. Comparing the direct method with the method of extrarelaxation iteration shows that the former is about 3 times faster than the latter.

The numerical integration is divided into two phases. In the first phase, the model is integrated for 10 years with the annual mean wind stress (Hellerman, 1968) and annual mean heat flux at sea surface (Haney, 1971) as the forcing boundary conditions. At the end of the 10th year, a quasi-equilibrium state of model climate in upper levels is reached. In the second phase, the initial condition is just the quasi-equilibrium state obtained above and then the model is integrated for one year with region-averaged (between 30°N, 160°E—140°W and 30°S, 150°E—90°E) wind stress both in winter (December—February) and in summer (June—July) (see Fig. 1), calculated by Wyrtki (1974). Besides, the annual mean heat flux is still used in the computation.

IV. RESULTS AND DISCUSSION

The temperature of the sea surface (represented by a 50 m layer from the sea level) and the vertical velocity under the sea surface layer in the first phase are shown in Fig. 2, which reveals the large-scale features of annual mean temperature of sea surface in the Pacific Ocean, e.g., sea water is warmer in the west part, and especially, the narrow cold tongue of sea water in the equatorial region extends westward. The cold tongue is supported by the corresponding strong vertical upwelling with a maximum value of 4.4×10^{-4} cm s^{-1}.

Similar temperature pattern is shown at the level of 250 m (figure not shown). The cold tongue of sea water is still in presence. The temperature of sea water is 13.2°C in the west and 12.5°C in the east. In middle latitude area the isotherms are smooth. The averaged temperature in the whole region is 12.8°C.

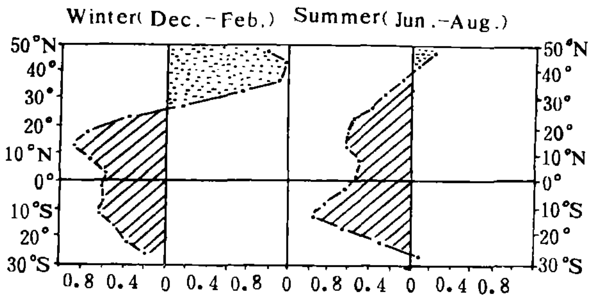

Fig. 1. Horizontal wind stress over the Pacific Ocean (Wyrtki, 1974).

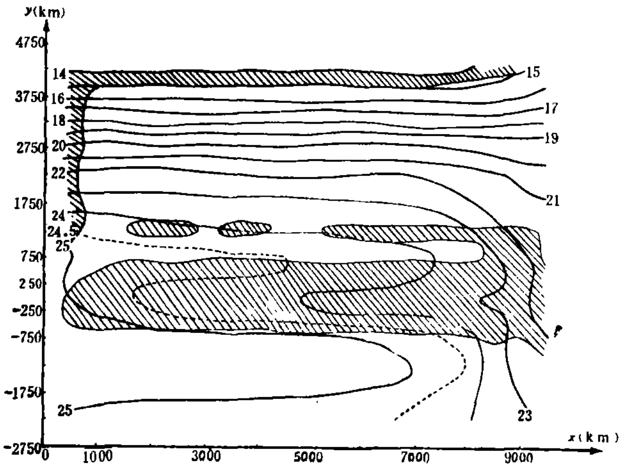

Fig. 2. Temperature T(°C) of sea surface (a 50 m layer) at the end of first phase (hatched area indicates upwelling below the sea surface).

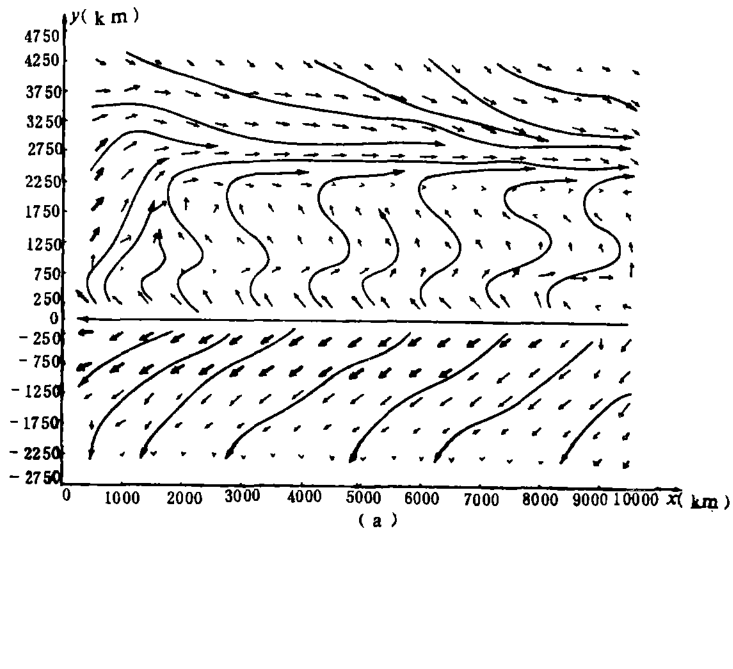

(a)

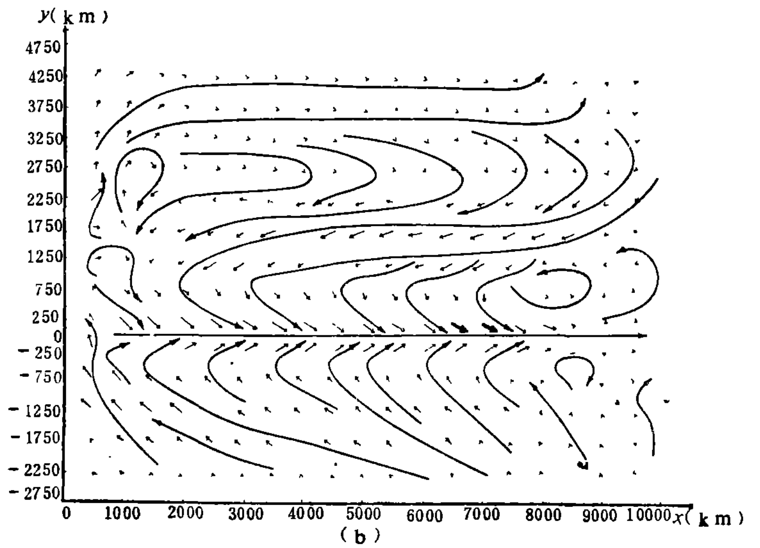

(b)

Fig. 3. Computed ocean currents at the end of the first phase: (a) at the 50 m sea surface layer and (b) at the 250 m layer.
The absolute magnitude of velocity $|V|$ is denoted by: angle marks $|V|<0.5$ cm s^{-1}; short arrows $0.5\leqslant|V|<1$ cm s^{-1}; moderate arrows $1\leqslant|V|\leqslant2$ cm s^{-1}; and bold arrows $|V|>2$ cm s^{-1}.

Figs. 3a and 3b show the simulated annual mean currents at the 50 m sea surface layer and the 250 m layer in the first phase, respectively. Some major currents can be clearly seen there, such as the surface west boundary current, north and south equatorial currents, and the north equatorial countercurrent between 10°N which runs eastward. The south equatoial current crosses the equator and extends to 5°N. In addition, a westward undercurrent along the equator is also clearly shown at the 250 m layer.

These results are similar to those computed by Haney (1974). Because the low horizontal resolution and high viscosity coefficient are assumed in the model, the computed current values become smaller and the width of undercurrent gets larger. Nevertheless, the major features of large-scale current in the tropical ocean are still obvious.

Table 2. Average Horizontal Velocity u at the Sea Surface in the East Area (cm s^{-1})

Current	North Equatorial Current	North Equatorial Countercurrent	South Equatorial Current					
Distance from Equator	1750 km	1250 km	750km	250km	−250km	−750km	−1250km	−1750km
Winter	−0.3	−0.2	−0.6	−4.0	−5.6	−2.3	−0.7	−0.1
Summer	−0.2	+0.1	−0.4	−3.9	−5.8	−2.6	−0.9	−0.1

Note: Symbol + means the eastward current, − the westward current.

The average current values in the east area in the second phase are listed in Table 2, in which the seasonal variation of countercurrents can be clearly seen. In winter when the north-east trade wind strengthens in the Northern Hemisphere, the countercurrent becomes weaker or even disappeared, but in summer it gets stronger. This result is in agreement with the observations made by Wyrtki (1965). The south equatorial current always crosses equator in both winter and summer. When located in the north of the equator, it is stronger in winter than in summer, while in the Southern Hemisphere it is stronger in summer than in winter. This is mainly caused by the north-east trade wind which is stronger in summer than in winter in the Southern Hemisphere.

The undercurrent of the equator is clear in both winter and summer. It runs eastward along the equator and has a width of about 500 km. The seasonal change of the undercurrent is not so clear as that of surface currents, but it can also be distinguished that the undercurrent gets weaker in summer and stronger in winter.

All results mentioned above show that the seasonal change of equatorial currents has a sensitive response to that of the trade wind.

Although many large-scale features of tropical oceans are simulated in this paper, some inadequacies, such as low horizontal and vertical resolutions, high viscosity coefficient and the neglect of seasonal change of heat flux, still need improving.

REFERENCES

Haney, R.L. (1971). Surface thermal boundary condition for ocean circulation model, *J. Phys. Oceanogr.*, **1**: 241—248.

Haney, R.L. (1974), A numerical study of the response of an idealized ocean to large-scale surface heat and momentum flux, *J. Phys. Oceanogr.*, **4**: 145—167.

Hellerman, S. (1967), An updated estimate of the wind stress on the world ocean, *Mon. Wea. Rev.*, **95**: 607—626.

Hellerman, S. (1968), An updated estimate of the wind stress on the world ocean, *Mon. Wea. Rev.*, **96**: 63—74.

Huany, J.C.K. (1979), Numerical simulation studies of oceanic anomalies in the North Pacific basin, II. Seasonally varying motions and structures, *J. Phys. Oceanogr.*, **9**: 37—56.

Lilly, D.K. (1965), On the computational stability of numerical solutions of time-dependent non-linear geophysical fluid dynamics problems, *Mon. Wea. Rev.*, **93**: 11—26.

Veronis, G. (1966), Wind-driven ocean circulation Part 2, numerical solutions of the non-linear problem, *Deep-Sea Research*, **13**: 31—55.

Wyrtki, K. (1965), The annual and semiannual variation of sea surface temperature in the North Pacific Ocean, *Limnol. Oceanogr.*, **10**: 307—313.

Wyrtki, K. (1974), Equatorial currents in the Pacific 1950 to 1970 and their relation to the trade winds, *J. Phys. Oceanogr.*, **4**: 372—380.